LANGMUIR

Article

pubs.acs.org/Langmuir

Sessile Nanodroplets on Elliptical Patches of Enhanced Lyophilicity

Ivan Dević,[†] Giuseppe Soligno,[‡] Marjolein Dijkstra,[§] René van Roij,[‡] Xuehua Zhang,[∥,†] and Detlef Lohse*[,†]

[†]Physics of Fluids Group, Department of Applied Physics and J. M. Burgers Centre for Fluid Dynamics, University of Twente, P.O. Box 217, 7500 AE Enschede, The Netherlands

[‡]Institute for Theoretical Physics, Center for Extreme Matter and Emergent Phenomena, Utrecht University, Leuvenlaan 4, 3584 CE Utrecht, The Netherlands

[§]Soft Condensed Matter, Debye Institute for Nanomaterials Science, Department of Physics, Utrecht University, Princetonplein 5, 3584 CC Utrecht, The Netherlands

[∥]Soft Matter and Interfaces Group, School of Engineering, RMIT University, Melbourne, VIC 3001, Australia

ABSTRACT: We theoretically investigate the shape of a nanodroplet on a lyophilic elliptical patch in lyophobic surroundings on a flat substrate. To compute the droplet equilibrium shape, we minimize its interfacial free energy using both Surface Evolver and Monte Carlo calculations, finding good agreement between the two methods. We observe different droplet shapes, which are controlled by the droplet volume and the aspect ratio of the ellipse. In particular, we study the behavior of the nanodroplet contact angle along the three-phase contact line, explaining the different droplet shapes. Although the nanodroplet contact angle is constant and fixed by Young's law inside and outside the elliptical patch, its value varies along the rim of the elliptical patch. We find that because of the pinning of the nanodroplet contact line at the rim of the elliptical patch, which has a nonconstant curvature, there is a regime of aspect ratios of the elliptical patch in which the nanodroplet starts expanding to the lyophobic part of the substrate, although there is still a finite area of the lyophilic patch free to be wetted.

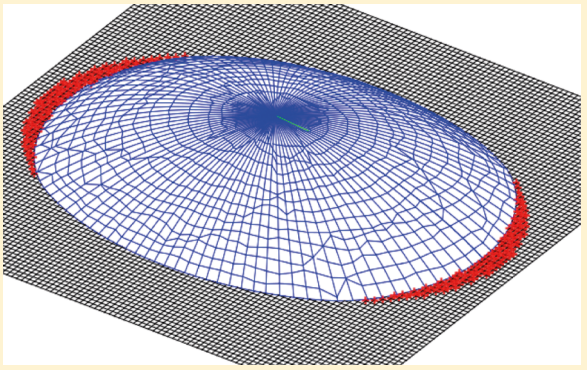

INTRODUCTION

Equilibrium shapes of nanodroplets, which are positioned on a patterned surface, are of great interest to both fundamental research[1−8] and many industrial applications such as printing,[9] microfluidics,[10] and catalysis.[11] If the nanodroplet is deposited on a homogeneous substrate, then it will form a spherical cap, with a contact angle dictated by Young's law. However, if we pattern the flat substrate with chemical heterogeneities, then the nanodroplet will no longer form a spherical cap but another equilibrium shape with constant mean curvature, which is determined by the Young−Laplace equation.[12] If the length scale of the chemical heterogeneities is much smaller than the length scale of the nanodroplet and if the heterogeneities are regularly and densely distributed over the substrate, then the nanodroplet has the apparent contact angle predicted by the modified Cassie−Baxter law.[13,14] However, when the chemical heterogeneities are on the same length scale as the nanodroplet itself, a strong coupling of droplet shape and surface heterogeneities emerges. In such a case, we have to numerically minimize the interfacial free energy of the nanodroplet because in three dimensions the minimization problem can often not be solved analytically.[15,16] The numerical techniques used in calculating the nanodroplet equilibrium shapes include the gradient descent method,[17,18] metropolis stochastic calculations,[19] hybrid energy minimizations,[20] and lattice Boltzman calculations.[21] Wetting experiments and calculations on isolated chemical defects, such as circular islands[22] and single stripes,[23−26] have shown that the contact angles along the three-phase contact line are determined by the local properties of the substrate, which will be discussed in more detail in the Results section.

In this article, we analyze the morphology of a nanodroplet on a single lyophilic elliptical patch on a flat substrate. The single elliptical patch is an intermediate case between a circular island and a single stripe, but it is qualitatively unique because the rim of the elliptical patch has a nonconstant curvature that affects the nanodroplet equilibrium shape and shape transformations via the Young−Laplace equation. In Figure 1, we show the possible nanodroplet states we expect to find in this system, which will be explained in more detail further on in the article. These states are analogous to those of the nanodroplet positioned on a single finite lyophilic stripe,[24] with the exception of the long cylindrical drops, which cannot be obtained because of the curvature of the rim of the elliptical

Received: January 18, 2017
Revised: March 1, 2017
Published: March 1, 2017

DOI: 10.1021/acs.langmuir.7b00002
Langmuir 2017, 33, 2744−2749

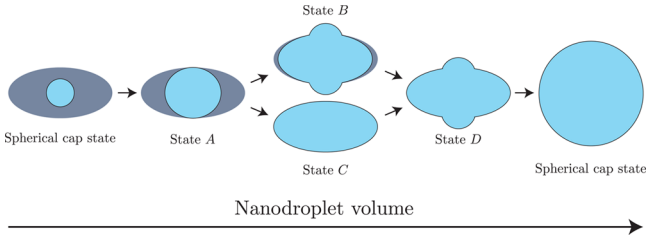

Figure 1. Graphical representation of all possible droplet states as seen from the top view.

patch. We expect two possible pathways, through either state B or state C, because the contact line of the nanodroplet has a tendency to pin itself in the region of the sharp transition of wettability (rim of the elliptical patch), which determines the value of one out of the two principal radii of curvature.

THEORETICAL DEFINITION OF THE PROBLEM

Because of the small size of a nanodroplet, we can neglect the effect of gravity. Moreover, for simplicity we ignore line tension contributions. Therefore, the shape of the nanodroplet is controlled by the surface tension among the three phases present in the system[27] (s, solid; l, liquid; and v, vapor). If the droplet is in contact with a flat substrate, described by the plane $z = 0$, with patterned chemical heterogeneities, then we can write the interfacial free energy E as

$$E = \gamma_{lv}A_{lv} + \int_{A_{sl}} (\gamma_{sl}(x, y) - \gamma_{sv}(x, y))\, dA \tag{1}$$

where γ_{ij} denotes the surface tension between phases i and j and A_{ij} represents the area of the interface between these two phases. Normalizing the interfacial free energy E with γ_{lv} and using Young's law for the contact angle

$$\cos\theta_Y(x, y) = \frac{\gamma_{sv}(x, y) - \gamma_{sl}(x, y)}{\gamma_{lv}} \tag{2}$$

we obtain the expression for a reduced interfacial free energy $\tilde{E}$

$$\tilde{E} \equiv \frac{E}{\gamma_{lv}} = A_{lv} - \int_{A_{sl}} \cos\theta_Y(x, y)\, dA \tag{3}$$

NUMERICAL METHODS AND PROCEDURE

We minimize eq 3 under the volume constraint to obtain the equilibrium shape of the nanodroplet. The geometry of our system is presented in Figure 2, where the origin of the coordinate system (x, y, z) is in the center of the elliptical patch, with large semiaxis a and small semiaxis b. We define ϕ as a viewing angle where the value zero corresponds to the direction of the x axis and $R(\phi)$ denotes the distance from the center of the elliptical patch, with which we will describe the contact line of the nanodroplet. We define the Young contact angle in our system as

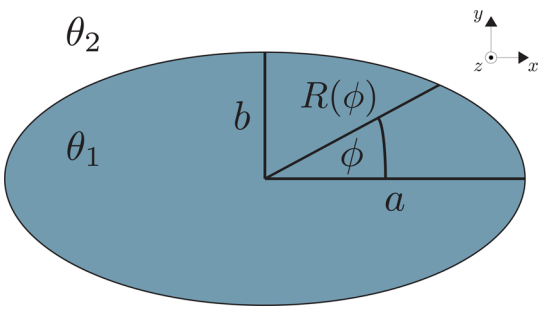

Figure 2. Geometry of an elliptical patch defined by semiaxes a and b, with Young's contact angle θ_1 inside the patch and θ_2 outside the patch.

$$\theta_Y = \begin{cases} \theta_1, \text{ if } (x, y) \in \dfrac{x^2}{a^2} + \dfrac{y^2}{b^2} \leqslant 1 \\ \theta_2, \text{ if } (x, y) \in \dfrac{x^2}{a^2} + \dfrac{y^2}{b^2} > 1 \end{cases} \tag{4}$$

where θ_1 is always smaller than θ_2, so the surface of the elliptical patch has an enhanced lyophilicity compared to the rest of the flat substrate.

We minimize eq 3 numerically with the Surface Evolver[17,18] and with Monte Carlo[19] calculations. Surface Evolver, developed by Brakke, is a free software package for minimizing the interfacial free energy; it was used with great success to calculate equilibrium wetting morphologies.[13,23,24,28,29] After setting the initial shape of the droplet, Surface Evolver triangulates the interface of the nanodroplet and moves the points of each triangle with an energy gradient descent method. The contact area A_{sl} is omitted from the Surface Evolver calculation, and we replace it with the integral of the second term of eq 3. In the Monte Carlo calculation, we use a simulated annealing method to calculate the global minimum of the interfacial free energy (eq 3), with the fluid−fluid interface represented by a grid of points. During the Monte Carlo simulation, a random shift in the morphology of the nanodroplet is introduced, and the interfacial free energy values (eq 3) before and after the shift are compared. If the value of the interfacial free energy is smaller after the shift, then we accept the new morphology. If it is larger, then we assign a probability of accepting the new morphology weighted by a temperature-like parameter T. This procedure is repeated continuously while T is gradually lowered, and the simulation ends when $T = 0$ (Metropolis algorithm).[19] In all of the presented calculations, we use the large semiaxis a as our unit of length, and we consider different aspect ratios b/a by tuning the small semiaxis b and different volumes V/a^3 of the nanodroplet. The values of the Young's contact angles in all calculations are set to $\theta_1 = 30°$ (lyophilic patch) and $\theta_2 = 60°$ (lyophobic surface). First, we position the nanodroplet center of mass above the center of the elliptical patch, and we set the nanodroplet initial volume to $V = 0.01a^3$. After calculating the nanodroplet equilibrium shape, i.e., corresponding to the minimum in the interfacial free energy, we increment the nanodroplet volume by $\Delta V = 0.01a^3$ and recalculate its equilibrium shape. We repeat this process until we reach $V = a^3$.

RESULTS

When the nanodroplet is sufficiently small to have the whole three-phase contact line inside the elliptical patch or when it is large enough to have the whole contact line outside the elliptical patch, the nanodroplet has a spherical-cap shape, with the contact angle defined by eq 4. We analytically calculate threshold volumes V_{min} and V_{max} of the nanodroplet, for which the nanodroplet is, respectively, too large to form the spherical-cap shape inside the patch or sufficiently large to form the

DOI: 10.1021/acs.langmuir.7b00002
Langmuir 2017, 33, 2744−2749

spherical-cap shape completely covering the elliptical patch, namely,

$$V_{\min} = \frac{b^3\pi}{3\sin^3\theta_1}(\cos^3\theta_1 - 3\cos\theta_1 + 2) \quad (5)$$

$$V_{\max} = \frac{a^3\pi}{3\sin^3\theta_2}(\cos^3\theta_2 - 3\cos\theta_2 + 2) \quad (6)$$

which correspond, using $\theta_1 = 30°$ and $\theta_2 = 60°$, to $V_{\min} \approx 0.431b^3$ and $V_{\max} \approx 1.007a^3$. For all values of the nanodroplet volume between threshold volumes $V_{\min}$ and $V_{\max}$, the nanodroplet will be in one of the following four possible morphologies:

- Droplet state A: the nanodroplet has a part of the three-phase contact line pinned at the rim of the elliptical patch, and the rest of the contact line is located inside the elliptical patch. As we increase its volume, the nanodroplet can evolve to droplet state B or C, depending on the aspect ratio of the elliptical patch.
- Droplet state B: the nanodroplet partially spreads outside the elliptical patch, although the elliptical patch (which is more lyophilic) is not fully wetted.
- Droplet state C: the whole three-phase contact line of the nanodroplet is pinned at the rim of the elliptical path.
- Droplet state D: part of the nanodroplet contact line is still pinned to the rim of the elliptical patch, and the rest of the contact line is outside of the elliptical patch. Both states B and C undergo a morphological transformation to state D once the volume has become sufficiently large.

In Figure 3, we present results for the equilibrium shapes of a nanodroplet on an elliptical patch of aspect ratio $b/a = 0.7$ as obtained from Monte Carlo simulations for varying droplet volumes V as labeled. The results as obtained from the Surface Evolver are very similar (Figure 4). We find that the shape transformation proceeds via droplet state C to state D as anticipated in Figure 1 upon increasing the droplet volume V.

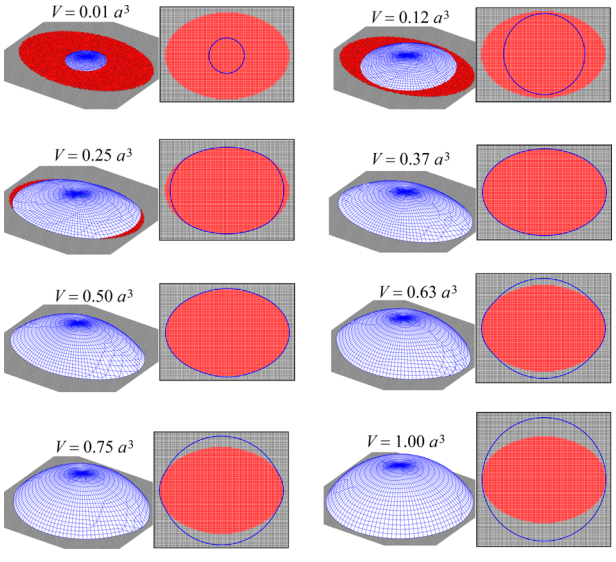

Figure 3. Equilibrium shapes (blue grid) of a nanodroplet with increasing volume on an elliptical patch (red area) with aspect ratio $b/a = 0.7$, as obtained from Monte Carlo calculations. The respective right figures show a top view of the three-phase contact line (blue line).

We now focus on the properties of the three-phase contact line and the local contact angle of the nanodroplet. In Figure 4, we show the position of contact line $R(\phi)$ and local contact angle $\theta(\phi)$ as a function of viewing angle ϕ for different volumes of the nanodroplet, corresponding to different droplet states. For the chosen aspect ratio of elliptical patch $b/a = 0.4$, the nanodroplet will undergo the transformation from droplet state A to state B, therefore avoiding state C. We notice from these results that along the contact line of the nanodroplet the local contact angle is exactly the Young's angle predicted from eq 4 if the contact line is locally either inside (θ_1) or outside (θ_2) the elliptical patch. However, when the contact line is exactly at the rim of the elliptical patch, Young's law cannot be obeyed[12,24] and the local contact angle has a value of between θ_1 and θ_2. Although Young's law cannot be obeyed, the net force exhibited on the nanodroplet is zero as a result of the inversion symmetry of the system with respect to the x and y axes. When the nanodroplet volume reaches the value of $V_{\min}$, the contact line starts touching the rim of the elliptical patch, and at this point, the local contact angle starts increasing and the nanodroplet transforms from state A to state B. As we further increase the volume of the nanodroplet, once the value of the local contact angle reaches θ_2, the contact line of the nanodroplet will locally leave the rim of the elliptical patch and will move outside the patch. Because the rim of the elliptical patch has a nonconstant curvature, the nanodroplet cannot have an equilibrium morphology where the local contact angle has a value of θ_2 and is constant along the contact line in regions where it is pinned to the rim. This fact determines whether the growing nanodroplet will go through state B or state C. For a given volume, when $R(90°) = R(270°) = b$ and $\theta(90°) = \theta(270°) = \theta_2$, if $R(0°) = R(180°) < a$, then the nanodroplet will undergo a morphological transition from state A to state B. Instead, if $R(0°) = R(180°) = a$, then the nanodroplet will be in state C. Both states B and C eventually go through the transition to state D. Once the nanodroplet volume reaches the value of $V_{\max}$, the nanodroplet equilibrium shape is a spherical cap with a Young's contact angle of θ_2.

We can study the transitions in a clearer way if we expand the function $R(\phi)$ into a (truncated) harmonic series as

$$\frac{R(\phi)}{a} = c_0 + \sum_{i=1}^{4} c_i \cos(2i\phi) \quad (7)$$

In Figure 5, we present coefficients from eq 7 as a function of the volume of the nanodroplet for three different aspect ratios, which represent three different scenarios of droplet states. As already mentioned, for the value of the aspect ratio of elliptical patch $b/a = 0.4$ (Figure 5a), the nanodroplet cannot wet the elliptical patch in state C, whereas for $b/a = 0.7$ (Figure 5b), the nanodroplet cannot be in state B, which is visible from constant coefficient values for different values of the volume of the nanodroplet. (The contact line has the same position for different values of the volume of the nanodroplet.) Once the value of coefficient c_1 reaches its global maximum, the nanodroplet goes through a morphological transition from state A to either state B or C, depending on the values of $R(0°)$ and $R(90°)$ when $\theta(90°)$ and $\theta(270°)$ reach θ_2. As the volume becomes larger, all of the higher harmonics go to zero because the nanodroplet becomes a spherical cap again.[22] We notice that for a circular patch, where $b/a = 1$ (Figure 5c), all of the higher harmonics remain zero for any volume of the nanodroplet because the nanodroplet has a spherical cap

DOI: 10.1021/acs.langmuir.7b00002
Langmuir 2017, 33, 2744−2749

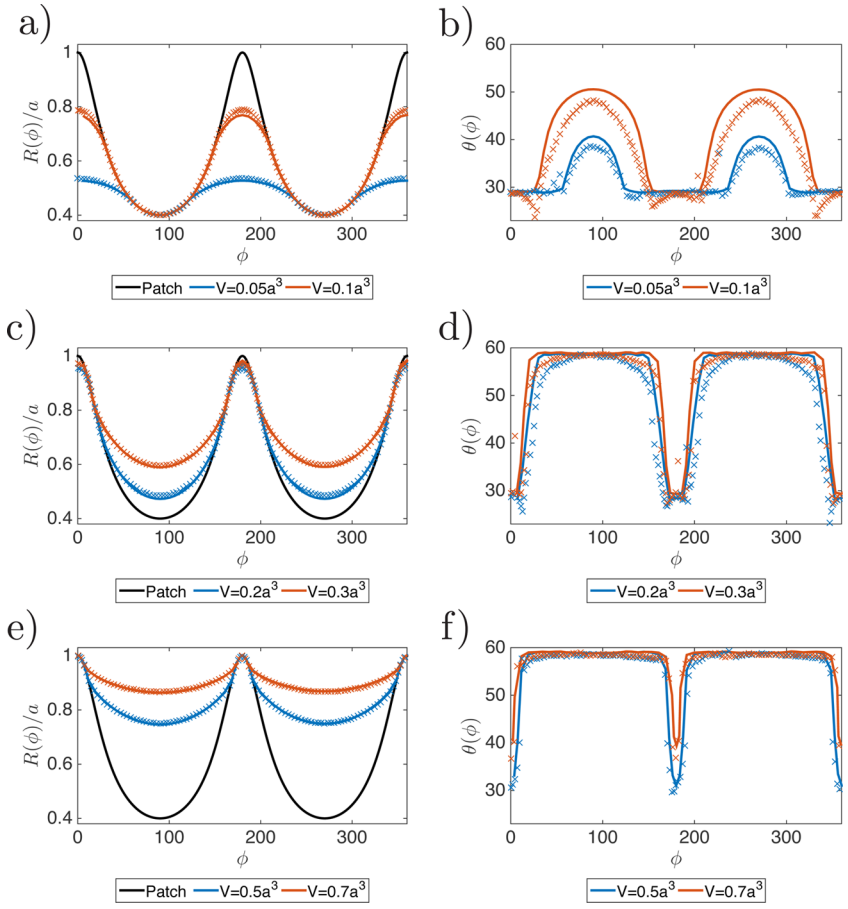

Figure 4. Position of contact line $R(\phi)$ and local contact angle $\theta(\phi)$ of the nanodroplet wetting an elliptical patch with aspect ratio $b/a = 0.4$ as a function of viewing angle ϕ and for varying droplet volumes as labeled. We show $R(\phi)$ and $\theta(\phi)$ (a, b) for the nanodroplet in state A, (c, d) for the nanodroplet in state B, and (e, f) for the nanodroplet in state D. Solid lines show the results from the Surface Evolver calculation, and the markers present results from the Monte Carlo calculations.

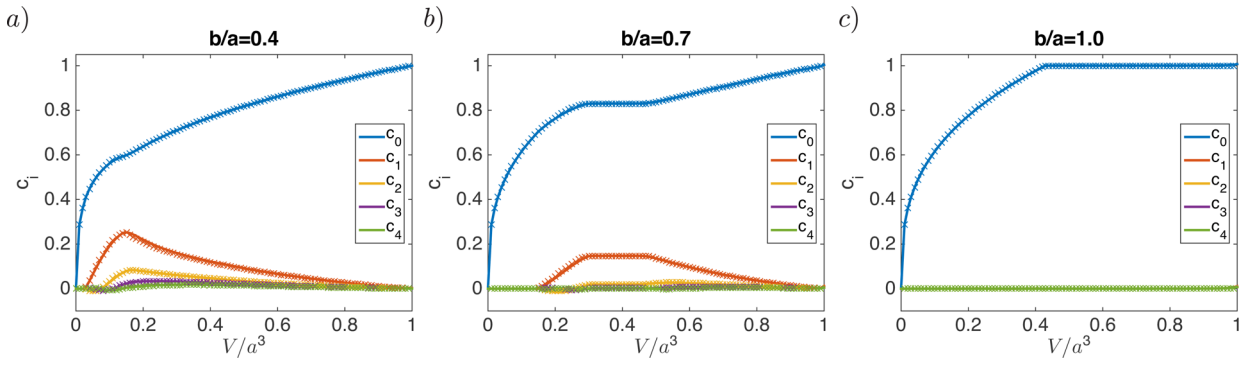

Figure 5. Expansion of $R(\phi)$ into a harmonic series as described in eq 7 for different values of the volume of the nanodroplet (V/a^3) and different aspect ratios of the elliptical patch: (a) $b/a = 0.4$, (b) $b/a = 0.7$, and (c) $b/a = 1$. The results are presented in the same way as in Figure 4: solid lines correspond to Surface Evolver calculations, and the markers correspond to the Monte Carlo calculations.

shape for any volume. Small deviations of the harmonics close to nanodroplet volume $V = a^3$ are a numerical artifact from Surface Evolver due to a complicated definition of the interfacial energy on the flat substrate for this particular system. We summarize all of our results in the state diagram presented in Figure 6, where we show the nanodroplet morphological states with respect to nanodroplet volume V and elliptical patch aspect ratio b/a. Note that the presented state diagram holds for inside-patch and outside-patch Young's contact angles given by $\theta_1 = 30°$ and $\theta_2 = 60°$, respectively, so it can be quantitatively different for other combinations of these two values.

CONCLUSIONS

We have calculated the equilibrium shapes of nanodroplets on elliptical patches of enhanced lyophilicity with two different numerical methods and have obtained good agreement between the two methods. With this work, we have connected the equilibrium shapes of a nanodroplet on isolated circular islands and the single stripe with all of the intermediate cases

DOI: 10.1021/acs.langmuir.7b00002
Langmuir 2017, 33, 2744−2749

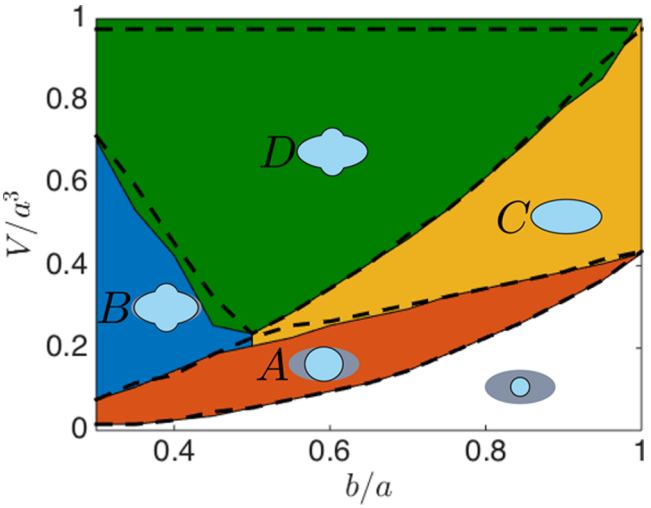

Figure 6. State diagram of the droplet morphologies as a function of aspect ratio b/a of the elliptical patch (with inside patch contact angle $\theta_1 = 30$ and outside patch contact angle $\theta_2 = 60$) and reduced volume V/a^3 of the nanodroplet. Solid lines present volume thresholds calculated in the Surface Evolver calculation, and dashed lines (in good agreement with the solid lines) present Monte Carlo results.

with varying aspect ratio b/a of the elliptical patch. We calculated all of the threshold volumes at which a morphological transition occurs for the given Young's angles ($\theta_1 = 30°$ and $\theta_2 = 60°$), which are summarized in Figure 6. The droplet states that we observe are similar to those reported on single lyophilic stripes.[23−25] However, because of the curvature of the rim of the elliptical patch, we do not observe long cylindrical drops on the elliptical patch. For practical applications of the elliptical patch, such as in catalysis, the separation of the aspect ratio of the elliptical patch into two regimes, either state B or state C, is an important result. If we think of chemical patterning as an investment in the substrate to be more efficient (isolation of a certain liquid on the patch), then the expansion of the contact line of the nanodroplet outside of the elliptical patch when there is still area available inside the elliptical patch is an inefficient way of patterning.

AUTHOR INFORMATION

Corresponding Author

*E-mail: d.lohse@utwente.nl.

ORCID

Ivan Dević: 0000-0003-0977-9973

Xuehua Zhang: 0000-0001-6093-5324

Detlef Lohse: 0000-0003-4138-2255

Author Contributions

I.D. and G.S. contributed equally to this work.

Notes

The authors declare no competing financial interest.

ACKNOWLEDGMENTS

G.S. and R.v.R. acknowledge financial support by Marie Curie Initial Training Network SOMATAI. This work was supported by The Netherlands Center for Multiscale Catalytic Energy Conversion (MCEC), an NWO Gravitation Programme funded by the Ministry of Education, Culture and Science of the government of The Netherlands. This work is part of the D-ITP consortium, a program of the NWO that is also funded by the Dutch Ministry of Education, Culture and Science (OCW). We are grateful to Ken Brakke for giving us advice in using Surface Evolver. We also thank S. Karpitschka and C. W. Visser for their insights on this work.

REFERENCES

(1) Marmur, A. Contact Angle Hysteresis on Heterogeneous Smooth Surfaces. *J. Colloid Interface Sci.* **1994**, *168*, 40−46.

(2) de Gennes, P. G.; Brochard-Wyart, F.; Quere, D. *Capillarity and Wetting Phenomena: Drops, Bubbles, Pearls, Waves*; Springer: New York, 2004.

(3) Quere, D. Wetting and roughness. *Annu. Rev. Mater. Res.* **2008**, *38*, 71−99.

(4) de Gennes, P. G. Wetting: statics and dynamics. *Rev. Mod. Phys.* **1985**, *57*, 827.

(5) Herminghaus, S.; Brinkmann, M.; Seemann, R. Wetting and Dewetting of Complex Surface Geometries. *Annu. Rev. Mater. Res.* **2008**, *38*, 101−121.

(6) Rauscher, M.; Dietrich, S. Wetting Phenomena in Nanofluidics. *Annu. Rev. Mater. Res.* **2008**, *38*, 143−172.

(7) Lohse, D.; Zhang, X. Surface Nanobubbles and Nanodroplets. *Rev. Mod. Phys.* **2015**, *87*, 981−1035.

(8) Mendez-Vilas, A.; Jodar-Reyes, A. B.; Gonzalez-Martin, M. L. Ultrasmall Liquid Droplets on Solid Surfaces: Production, Imaging, and Relevance for Current Wetting Research. *Small* **2009**, *5*, 1366−1390.

(9) Soltman, D.; Smith, B.; Kang, H.; Morris, S. J. S.; Subramanian, V. Methodology for Inkjet Printing of Partially Wetting Films. *Langmuir* **2010**, *26*, 15686−15693.

(10) Lee, T.; Charrault, E.; Neto, C. Interfacial slip on rough, patterned and soft surfaces: A review of experiments and simulations. *Adv. Colloid Interface Sci.* **2014**, *210*, 21−38.

(11) Clausen, B. S.; Schiøtz, J.; Gråbæk, L.; Ovesen, C. V.; Jacobsen, K. W.; Nørskov, J. K.; Topsøe, H. Wetting/ non-wetting phenomena during catalysis: Evidence from in situ on-line EXAFS studies of Cu-based catalysts. *Top. Catal.* **1994**, *1*, 367−376.

(12) Lenz, P.; Lipowsky, R. Morphological Transitions of Wetting Layers on Structured Surfaces. *Phys. Rev. Lett.* **1998**, *80*, 1920−1923.

(13) Brandon, S.; Haimovich, N.; Yeger, E.; Marmur, A. Partial wetting of chemically patterned surfaces: The effect of drop size. *J. Colloid Interface Sci.* **2003**, *263*, 237−243.

(14) Marmur, A.; Bittoun, E. When Wenzel and Cassie Are Right: Reconciling Local and Global Considerations. *Langmuir* **2009**, *25*, 1277−1281.

(15) Gao, L.; McCarthy, T. J. How Wenzel and Cassie Were Wrong. *Langmuir* **2007**, *23*, 3762−3765.

(16) McHale, G. Cassie and Wenzel: Were They Really So Wrong? *Langmuir* **2007**, *23*, 8200−8205.

(17) Brakke, K. A. The Surface Evolver. *Exp. Math.* **1992**, *1*, 141−165.

(18) Brakke, K. A. *Surface Evolver Manual*, version 2.70; 2013; http://facstaff.susqu.edu/brakke/evolver/downloads/manual270.pdf.

(19) Soligno, G.; Dijkstra, M.; van Roij, R. The equilibrium shape of fluid-fluid interfaces: Derivation and a new numerical method for Young's and Young-Laplace equations. *J. Chem. Phys.* **2014**, *141*, 244702.

(20) Matsui, H.; Noda, Y.; Hasegawa, T. Hybrid Energy-Minimization Simulation of Equilibrium Droplet Shapes on Hydrophilic/Hydrophobic Patterned Surfaces. *Langmuir* **2012**, *28*, 15450−15453.

(21) Dupuis, A.; Léopoldès, J.; Bucknall, D. G.; Yeomans, J. M. Control of drop positioning using chemical patterning. *Appl. Phys. Lett.* **2005**, *87*, 024103.

(22) Extrand, C. W. Contact Angles and Hysteresis on Surfaces with Chemically Heterogeneous Islands. *Langmuir* **2003**, *19*, 3793−3796.

(23) Darhuber, A. A.; Troian, S. M.; Wagner, S. Morphology of liquid microstructures on chemically patterned surfaces. *J. Appl. Phys.* **2000**, *87*, 7768−7775.

DOI: 10.1021/acs.langmuir.7b00002
Langmuir 2017, 33, 2744−2749

(24) Brinkmann, M.; Lipowsky, R. Wetting morphologies on substrates with striped surface domains. *J. Appl. Phys.* **2002**, *92*, 4296−4306.
(25) Ferraro, D.; Semprebon, C.; Tóth, T.; Locatelli, E.; Pierno, M.; Mistura, G.; Brinkmann, M. Morphological Transitions of Droplets Wetting Rectangular Domains. *Langmuir* **2012**, *28*, 13919−13923.
(26) Jansen, H. P.; Bliznyuk, O.; Kooij, E. S.; Poelsema, B.; Zandvliet, H. J. W. Simulating Anisotropic Droplet Shapes on Chemically Striped Patterned Surfaces. *Langmuir* **2012**, *28*, 499−505.
(27) Woodward, J. T.; Gwin, H.; Schwartz, D. Contact Angles on Surfaces with Mesoscopic Chemical Heterogeneity. *Langmuir* **2000**, *16*, 2957−2961.
(28) Seemann, R.; Brinkmann, M.; Kramer, E. J.; Lange, F. F.; Lipowsky, R. Wetting morphologies at microstructured surfaces. *Proc. Natl. Acad. Sci. U. S. A.* **2005**, *102*, 1848−1852.
(29) Chen, Y.; He, B.; Lee, J.; Patankar, N. A. Anisotropy in the wetting of rough surfaces. *J. Colloid Interface Sci.* **2005**, *281*, 458−464.

DOI: 10.1021/acs.langmuir.7b00002
Langmuir 2017, 33, 2744−2749